J14.4 NUMERICAL SIMULATION INTERACTION BETWEEN DROP AND ICE PARTICLES AND ITS INFLUENCE ON FORMATION OF STRONG PRECIPITATION

Ganna Pirnach[1*], Taras Belyi[2]
[1]Ukrainian Hydrometeorological Institute, Kyiv, Ukraine
[2]Institute of Geophysics, NAS of Ukraine, Kyiv, Ukraine

1. INTRODUCTION[1]

Present work continues theoretical studies of heavy precipitation caused floods and damages in mountain regions of Ukraine. In recent years heavy precipitation causes flash floods in Carpathians region very frequently. According to [2] catastrophic sums of rainfall reach 237 mm/12h during floods. Cases of strong shower heavy convective and long lasting precipitation (as example in July of 1969, November of 1998, July of 2008) have been investigated in [1-3 , 5 , 7 , 8 , 11].

Three-dimensional nowacasting and forecasting numerical models developed in UHRI were adapted for theoretical interpretation of the investigated phenomena. Relative role of different mechanisms of cloud and precipitation formation and relative role of cloud drops, raindrops, crystals, ice nuclei, cloud condensation nuclei have been subjected for investigation [9].

RESEARCH METHODOLOGY

The three-dimension diagnostic and prognostic models with non-elastic dynamics at detail microphysics have been adapted for theoretical interpretation of the investigated phenomena. There is proposed research methodology based on numerical integration of dynamic and thermodynamic full equation jointly with kinetic equation for cloud particles distribution function. The system of equations and detail description developed algorithm its integration given in [3, 6, 9]. In this work particular attention will be devoted to the numerical experiments with spectra of cloud and precipitation particles of different phase state. Numeral simulation for the study of relative role of processes of condensation, coagulation and nucleation was conducted by the including or excluding of these processes.

Kinetic equation for cloud particle distribution functions described as follows:

$$\frac{df_1}{dt} = -\frac{\partial}{\partial r}(\dot{r}_1 f_1) + \frac{v_1}{G_0}\frac{\partial f_1}{\partial z} + I_a - I_{f1} - (c_{21} + c_{31}) f_1 + \Delta f_1$$

$$\frac{df_2}{dt} = -\frac{\partial}{\partial r}(\dot{r}_2 f_2) + \frac{v_2}{G_0}\frac{\partial f_1}{\partial z} - I_{f2} - \frac{\partial}{\partial r}\left(\dot{r}_{c_{21}} f_2\right) + \Delta f_2$$

$$\frac{df_3}{dt} = -\frac{\partial}{\partial r}(\dot{r}_3 f_3) + \frac{v_3}{G_0}\frac{\partial f_3}{\partial z} - \frac{\partial}{\partial r}\left(\dot{r}_{c_{31}} f_3\right) + I_s + I_{f1} + I_{f2} + \Delta f_2 \qquad (1)$$

t is time; r_i is radiuses of cloud and precipitation particles; x, y, z axis are directed on east, north and perpendicular to the ground surface respectively; $i = k = 1$ is for droplets; $i = k = 2$ is for crystals; $j = 1$ and $k = 3$ is for raindrops; f_i and f_j are cloud and precipitation particles size distribution functions; r_{ci} is rate of continuous coagulation growth of precipitation particles; functions $I_a, I_s, I_{f_1}, I_{f_2}$ describe of nucleation processes (generation on the cloud condensation nuclei (CCN), ice nuclei (IN), cloud droplets and precipitation drops, respectively); v_i is velocity of falling particles.

Operators df_i/dt and Δf_i are advection and turbulent transfer respectively; G_0 is relief factor [6 , 9].

The processes of formation of drops on the cloud condensation nuclei and ice nuclei calculated as [3, 9]. The processes of coagulation calculated at approaching to continuous growth.

In the kernel of gravitation collection coefficients of accretion for liquid precipitation are calculated as in [10]:

$$E_r = E_1\left[1 - \frac{r_2 r_m^3}{4r_1^2\left(r_2^2 - r_1^2\right)}\right]^2. \qquad (2)$$

r_1 is small drop radius, r_2 is radius of large drop, $r_m = 14.5\,\mu\text{m}$. Excepting of special experiments $E_1 = 1$ for drop. $E_r = 1$ for ice particles.

* *Corresponding author address:* Ganna M. Pirnach, Ukrainian Hydrometeorological Institute, Dept. of the Atmosphere Physics, Kiyv, Ukraine, 03028; e-mail: hanna@uhmi.org.ua.

As intensity of above-named processes to a great extent is determined by gradients of temperature, the series of numeral experiments were conducted with the artificial falling or growth of the surface temperature in the process of evolution. The additional gradient of temperature was added in equation for a surface temperature. It allowed strengthening and weakening the process of cloud and precipitation formation.

$$\frac{\partial T}{\partial t} = -T_s \cdot \tag{3}$$

$$T_s = a_T \cos\left(\frac{\pi t}{2T_a}\right), \tag{4}$$

where T_a, a_T are parameters which regulate the size of gradient and period of change of his sign are set. A formula was used also:

$$T_s = a_T t \cdot \tag{5}$$

Initial fields of meteorological variables are constructed using diagnostic models developed in UHRI [9]. Radio sounding data of BADC (British Atmospheric Date Centre) are used to construct of this field. Aerological information of the stations of Ukraine and nearby countries served as initial data. The drop and ice sizes distribution functions either equaled a zero or calculated by Khrigian-Masin distribution in the ice saturation region [11].

Diagnose of initial atmospheric state

Present work continues theoretical studies of heavy precipitation caused floods and damages in mountain regions of Ukraine. The investigation by diagnostic model is its essential part. Space distribution of various meteorological characteristics were calculated and analyzed. The term 23 30 GMT of July 24 2008 was selected for detail analyses. Three-dimensional meteorological fields were built for the chosen territory which included Ukrainian Carpathians.

In the selected time Carpathians mountain range was under the influence of the warm front located almost perpendicular to the ridge at latitude Uzhgorod. Warm frontal air mass was located in north of the front (Fig. 1). Warm air dominated also along the Eastern Carpathians to the east of it. According to the synoptic chart over Ukraine was area of low pressure with low gradients. According to satellite image, the western, central and south parts of Ukraine were cover powerful clouds.

In fig.1 the initial fields for two space grid resolutions shown. In first case (Fig.1, Row 1) horizontal steps in nested grid was equal $dx = dy = 10$ km; in second case it was $dx = dy = 5$ km (Fig.1, Row 2). Grid step for z was $dz = 150$ m in whole range $0 < z < 11$ km. In stretched grid $dx = dy = 100$ km. They used for boundary conditions initialization only.

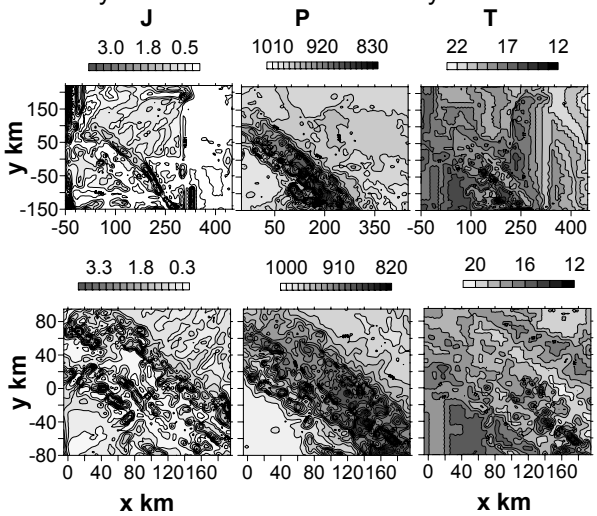

Fig. 1 Initial characteristics of clouds J are condensation rate comparable to the intensity of precipitation, mm/h.; P is pressure, hPa; T is temperature, C^o. First row: the spatial resolution of nested grid with steps $dx = dy = 10$ km. Second row: with $dx = dy = 5$ km. Coordinate origin $(x, y) = (0,0)$ is Uzhgorod.

Numerical experiments with different horizontal steps showed a large horizontal inhomogeneity of meteorological characteristics. Increase grid steps resulted in the loss of many vortex and cloud formations, and to reduce the vertical movements, and loss of other important microphysical and mesoscale structures of small scales.

Surface pressure field had closed area of low pressure to the north east and closed high-pressure cells in it. This area was characterized by the presence in it of precipitation of different intensity, showers and thunderstorms. Vertical movements have the cell structure and chains of updraft cells aligned along ridge.

Ice saturation was found only outside of a nested grid in the form of bands and individual spots. In the west, it occupied a wider area and initial distribution of cloudiness and precipitation in regions of saturation largely determine the behavior of clouds and precipitation in the nested grid. Measurement precipitation dropped out mainly outside the nested grids: In the west they were more widespread, and in the east manifested in the form of showers and thunderstorms. In the mountains they occur in small bands or spots on scales of several kilometers on both sides of the warm front.

Chain of cells of heavy precipitation stretches along the East Carpathians with the catastrophic amount within.

The chain of vortices in the atmospheric front extended perpendicular to the front on both sides of the ridge. The two chain vortices cells stretched along of the front line. They were cyclonic in cold air mass and anticyclonic in warm mass.

Condensation rate, vertical movements and total precipitation derived from the network measuring correspond to the configuration of vortices. Chain showers with the largest amounts of precipitation that observed in nature in the Carpathian region correspond to the chain of anticyclonic eddies and updraft cells.

Cloud and precipitation evolution under the mutual influence of particle spectra of different phase

Numerical experiments carried out to identify the features of the evolution of rain, which caused heavy floods in Carpathian Mountains. They focused on the features of the evolution of microphysical properties of clouds. Experiments were carried out using nested grids with horizontal separation step of 5 km (Fig. 1, second row).

In Fig. 2 shows the spatial distribution of temperature and pressure at t = 2 hours. The calculation corresponds to Line 8 of Table 1. As seen from the figure, pressure and temperature have spotted structure. The most noticeable area of high pressure and temperature have place in the north-east region. Plus, it holds a very strong inversion. This blocking process is obviously played a large role in the formation of some showers and thunderstorms that are observed in the west region. Warm air also spread in the hills. Warm front crossed the mountain ridge and was placed almost perpendicular to it. In Fig. 2 it is a part of air mass, placed near the coordinates y = 0 on both sides from the ridge. There were chains of eddies, as along the front and perpendicular to it.

The main goal of the first series of numerical experiments has been to find the most dangerous combinations of precipitation formation mechanisms that have been given catastrophic precipitation in region, associated with atmospheric fronts.

The following mechanisms involved in precipitation formation are as follows: the sublimation (redistribution of water vapor from drop to crystal as Findayzen–Bergeron mechanism); condensation growth of cloud drops; rain drop growth by gravitation coagulation in the approximation of continuous growth; freezing of drops; riming (coagulation of crystals with drops).

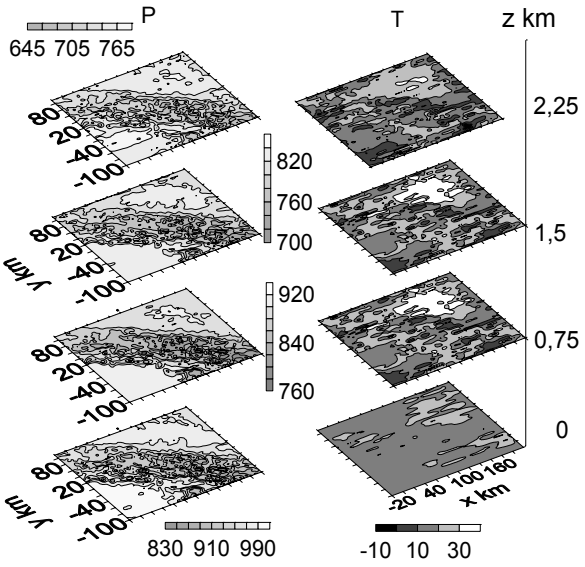

Fig. 2 Spatial distribution of pressure, P, hPa, temperature, T, C^{o}

In Table 1 and Fig. 3 the evolution of precipitation amounts at different mechanisms of precipitation formation and different initial conditions presented. The initial distribution of microphysical properties requires ice saturation presence. It is directly were not recorded over the investigating mountain regions in nested grid. But its probability of existence in individual cells was quite high due to penetration of water vapor as the east and west along with drop and crystals. They formed there, especially in the west and south, where the ice saturation covered a rather wide range. To the northeast of the nested grid the ice saturation also observed, but little more fragmented. To more clearly highlight the evolution of microphysical characteristics was conducted series of experiments with zero initial conditions, which helped to more clearly define the role of different mechanisms in the formation of catastrophic rainfall and strong precipitation.

Initial conditions influence on the whole future development of precipitation intensity and precipitation amounts. Comparison Cases 1 and 11, 2 and 8 and 5 and 6 of Table 1 and Fig. 4 let to notice that the nonzero initial distribution of droplets and crystals leads to a reduction of maximum rainfall amounts and distribution of rainfall in a wider area if coagulation drops with the drops activated.

Comparing Cases 3 and 9, when the coagulation process off, you may notice a

Table 1*

Evolution of 3-hour maximal sums in area $50 < x < 170$ km and $-60 < y < 30$ km at different mechanisms of cloud and precipitation formation

№	c_0	c_1	c_2	c_3	c_4	t h				
						3	6	9	12	Σ_0^{12}
1	1	0	0	1	1	3,8	4,1	3,8	3,6	15.3
d						0,0	0,2	2,7	3,0	6,9
2	1	1	1	1	1	3,8	4,6	6,1	3,6	18.1
d						0,0	2,8	6,1	0,0	8,9
3	1	0	1	1	1	3,8	4,1	3,8	3,5	15.2
d						0,0	0,3	2,2	1,3	3,8
4	1	1	1	0	1	3,8	6,8	16.5	3,6	30.7
d						0,0	6,8	16.5	0,1	23.4
5	1	1	0	0	0	3,8	5,3	10.2	3,6	22.6
d						0,0	5,3	10.2	0,0	15.5
6	0	1	0	0	0	0,0	12.	52.7	6,3	70.6
d						0,0	12.	52.7	6,3	70.6
7	0	0	0	0	0	0,0	0,2	1,3	1,2	2,7
d						0,0	0,2	1,3	1,2	2,7
8	0	1	1	1	1	0,9	9,1	35.8	0,9	48.7
d						0,0	9,1	35.8	0,9	47.8
9	0	0	1	1	1	0,0	0,3	3,3	0,9	4,5
d						0,0	0,2	3,3	0,9	4,4
10	0	1	0	1	1	0,9	5,3	14.1	7,0	27.3
d						0,1	5,3	14.1	6,5	26.0
11	0	0	0	1	1	0,0	0,3	1,3	0,9	2,5
d						0,0	0,1	1,3	0,9	2,3
12	0	1	1	1	0	0,0	4,6	4,6	2,4	11.8
d						0,0	4,6	4,6	2,4	11.8

*c_0 is identified a initial condition for cloud particles; c_1 is coagulation of large drops with small; c_2 is riming; c_3 is sublimation; c_4 is freezing; t is finish term of sums $c_i = 0$ (i = 0,1,2,3,4) are process excluded. Letter d presented large drops.

evident decreasing of total maximum amounts of precipitation and a slight increasing of a large drop part by its condensation growth. Cases 1 and 11 show the main contribution to the intensity of precipitation in the absence of crystals in the initial moment also the large drops make. With the introduction of artificial crystal the precipitation intensity increases mainly due to the ice fraction. Excluding the mechanism of formation of crystals by IN led to increase of precipitation amounts, especially of a large drop fraction. Excluding all mechanisms of ice formation led to catastrophic amounts of precipitation (Case 6).

Comparing Cases 6 and 8 with the strongest rainfall, we can conclude that the presence of ice reduces the probability of catastrophic rainfall, especially in the absence of riming (Case 10), thus expanding the territory of their falling. Excluding of the freezing processes also dampened precipitation intensity (Cases 4 and 5, 8 and 12).

Characterizing the relative role of drop and crystal fractions in precipitation of different intensity (Fig. 3, Table 1), should mark a decisive role of large drop fraction in the formation of catastrophic precipitation. In all the examining cases, the largest maximum amounts of precipitation was obtained for rain clouds, when all mechanisms of ice formation were excluded (Case 6). Second maximum was obtained when all precipitation formation mechanisms were included and zero initial conditions were used (Case 8). Despite the fact that all the mechanisms involved, precipitation has provided almost exclusively by large drop fraction.

According to Table 1 (Rows 2, 4, 5, 12) processes of solid phase nucleation cut heavy precipitation and freezing processes increased it.

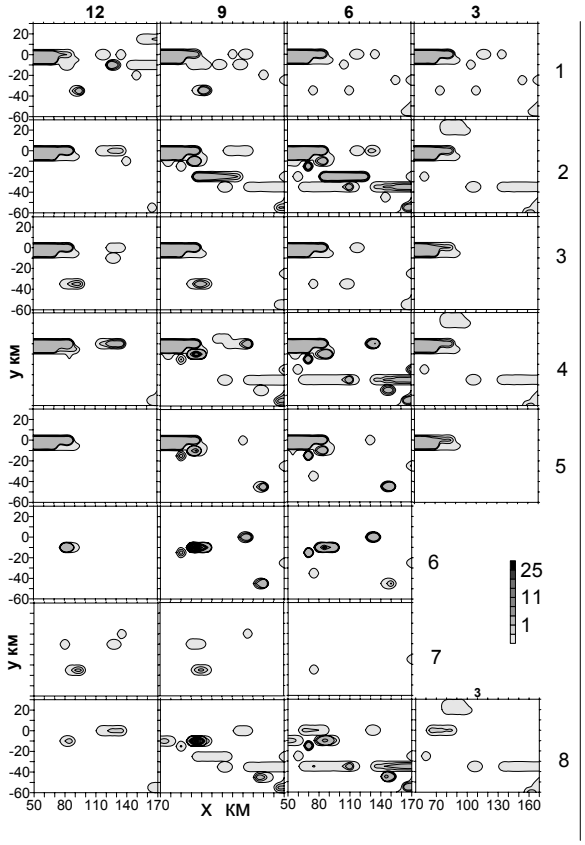

Fig. 3. Evolution of the amounts of precipitation at different mechanisms of clouds and precipitation formation
Row numbers correspond to numbers of rows in Table 1. Numbers near scales are 3-hour amounts, mm. Numbers near the tops of pictures are their deadlines.

Obviously, the formation ice with nucleation nuclei led to a large number of small solid particles that are taken on a lot of water vapor and this slowed rapid growth of precipitation particles. Reducing the number of raindrops by freezing caused by rapid growth the rest of drops to large sizes, which allowed them to fly through the unsaturated water vapor layers and do not evaporate.

Coagulation crystals and drops in the absence of coagulation of drops with the drops could significantly increase the amount of precipitation, but not catastrophic (Cases 9, 11). Rainfall in these cases dropped in separate spots and their precipitation cores placed in rain areas. Often the intensity of rain determined droplets spectra even in the absence of coagulation processes drops with drops. This precipitation is short–term. They occupy small areas but their intensity can reach significant values (i.e., Cases 9, 11).

Fig. 4 displays the maximum intensity in a target area of precipitation and the mean value within the area of their falling and the values of these quantities for the large drop fraction.

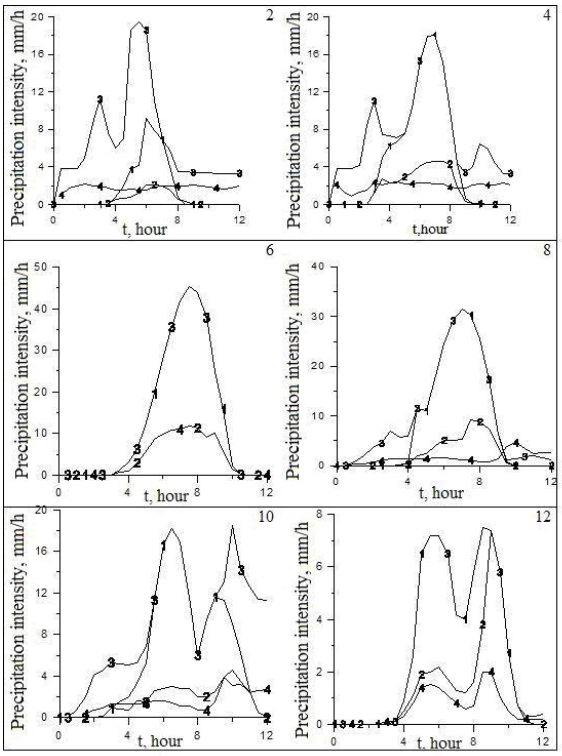

Fig.4. Precipitation intensity
Numbers in tops correspond to rows of Table 1. Numbers near lines: 1 is maximal intensity of drop precipitation: 2 is mean intensity of drop precipitation; 3 is maximal precipitation intensity; 4 is mean precipitation intensity.

Selected cases of heavy rain (Cases 2 and 4, Row 1 in Fig. 4) demonstrate the role of different mechanisms for the origin of ice on the intensity of heavy precipitation. Excluding of ice nucleation mechanism led to increased amounts of precipitation, although the maximum intensity has changed little.

Average intensity of large drop fraction access these values for total intensity. That means that the large drop heavy precipitation was concentrated on a smaller area. Excluding all the mechanisms of formation of crystals resulted in maximal increasing of precipitation intensity compared to all cases. Greatly increased and the average precipitation intensity, but sharply decreased area occupied by them (Fig. 3).

Comparing Case 2 and Case 8, which differ only by initial conditions, can be noted that the maximum intensity increased significantly, and very heavy precipitation concentrated in a smaller area at nonzero initial condition,.

In the Case 10, compared with Case 8, were excluded riming. The intensity of heavy rainfall in the latter case, decreased in size, but expanded space and time of falling

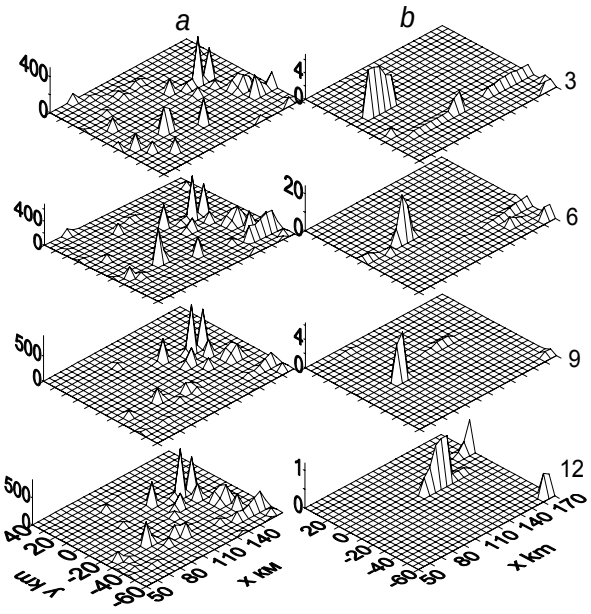

Fig. 5 Evolution of cloud and precipitation, Case 8, *a*: total Z-integral of water and ice, 10^{-3} mm, b: intensity of rainfall, mm/h. Numbers near pictures are time, h

In Fig. 5 shows the evolution of clouds and rain within 12 h development. Clouds composed of many individual convective cells. Under ridge cloud covers was almost no presenting. The largest cloud covers and largest precipitation cover observed in the East Carpathian Mountains. The most intense precipitation was observed in the cell, which operated in our region for nearly 6 hours. The highest intensity of rainfall was received at *t* = 7 h and reached 31.5 mm/h.

Paying attention to the fact that the total average rainfall intensity is no greater than the drop fraction, we can note that the role of crystal precipitation fraction in epicenters not increased. Riming of drops (Case 8) reduced the concentration of drops, and the rest of drops had more favourable conditions for its growth and rapidly falling. Exclusion of freezing drops sharply reduced the amount and intensity of precipitation, almost eliminating ice phase of the process of precipitation formation. Judging from the distribution of mean values, core of strong drop precipitation narrowed and a drop faction played a dominant role in the distribution of precipitation.

The most intense rainfall in the target point Fig. 6 located near the epicenter of precipitation for Case 6 was obtained around *t* = 8 hours (about 11 hours of local time). In less productive mechanisms of heavy precipitation is falling dawn earlier and shorter time.

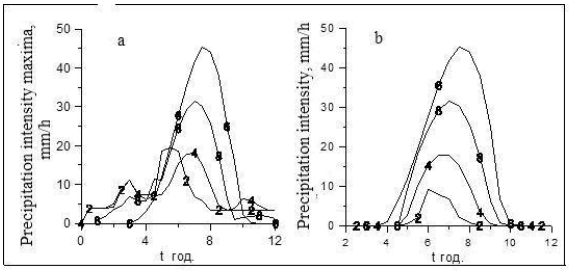

Fig. 6 The evolution of precipitation in their epicenters
a: maximum intensity of rainfall in a target area. b: precipitation intensity in a target point $(x\,;y)=(85;-10\,\mathrm{km})$. The symbols 0 and * denote the Case 10 and Case12 respectively.

The next series of experiments was devoted to research depending on precipitation of boundary conditions and vertical separation of the computing grid. The relative roles of the condensation and coagulation processes in the formation of dangerous precipitation have been identified.

Table 2
Evolution of the maxima on a target area of precipitation amounts at various boundary conditions and various computer grid resolutions

№	*L*	*ds*	C_W	C_1	C_2	*t*, h				$\sum_0^{12}$
						3	6	9	12	
1	0	150	1	0	0	0,1	5,5	30	50	90
2	1	200	1	0	0	0,1	2,1	7,5	20	30
3	1	200	1	0	1	0,0	2,6	7,5	3,5	15
4	1	200	1	1	1	13	38	55	45	161
5	2	200	1	0	0	0,0	1,5	4,2	3,0	8,7
6	2	200	1	1	1	0,9	19	40	60	120
7	2	200	0	1	1	0,7	21	11	0,6	33

Row 1: $dz=150$ m ($L=0$), rows 2; 3; 4: $dz=200$ m, above the tropopause continuity equation was excluded ($L=1$); rows 5; 6; 7: continuity equation was included everywhere $(L=2)$; row 6: excluded condensation (evaporation) rain drops $(c_w=0)$; $c_1=0$ is excluded coagulation of drops; $c_2=0$ is excluded coagulation of crystals with drops.

In Table 2 it is shows the results of experiments with calculations for the different vertical stratification for vertical movement. The boundary conditions for the temperature of the earth were modified using the relation (5); $a_T=2$. It caused the permanent fall of temperature, which in turn intensified the condensation and sublimation growth of cloud

particles and precipitation amounts. This regularity is disturbed only exception of the process of condensation of large droplets in the presence of coagulation of drops (Row 7) or exclusion of coagulation (Row 3). In these cases, the clouds would reaches to unstable equilibrium and a wave process occurs within the calculated time.

Correct calculation of the vertical movement at the stratification of the atmosphere on physical characteristics and use of continuity equations for all layers in the absence of processes coagulation has also led to a similar behavior of investigated phenomena (Row 5). In other cases, at a target temperature distribution even the absence of coagulation processes can not stop the growth of precipitation amounts to catastrophic (e.g., Row 1 and Row 2 in Table 2). If both coagulation processes operate together with the processes of condensation and sublimation, the increase precipitation amounts to catastrophic rainfall provided with high probability (Row 4 and Row 6 of Table 2).

The difference between the values of the sums of the first and second rows can be explained by the large number of small crystals in the cloud tops that penetrated in the tropopause. These crystals are falling down in lower layers, creating competition for growth drops, slowing it.

Thus, the dynamics and microphysical processes are competing with each other, and can create an unstable equilibrium in the clouds, and the disturbance of it may cause catastrophic precipitation.

In Table 3 shows the dependence on the amounts of precipitation of the width of the spectra of rain drops. *a* is geometric progression factor for the growth step integration of rain drops along the radius. *R* is raindrop radius maximum, microns. The calculations were carried out without regard to coagulation processes. Step of integration *dr* for large drop increased from *dr* = 20 microns (maximum radius of the smallest drops) with *a* - factor. As shown in Table 3 with increasing R (expanding of spectra of rain drops), precipitation increases to a certain size and then widening the spectra is leading to a certain equilibrium, apparently caused by an interaction of dynamical and microphysical processes. Further calculations were carried out with the value *a* = $\sqrt{2}$, which were obtained at the maximum amount of precipitation.

Calculations considering the processes of coagulation and using of different values of E_r showed that the most probability to receive catastrophic rainfall using formula (2). As shown by further calculations, just use this formula leads to the rapid collapse in the process of precipitation formation. Since in this case the largest coagulation factor is for the largest drops in size, it is evident that the redistribution of moisture in favor of the largest drops leading to undue expansion of the spectra and catastrophic fallout.

Table 3

Evolution of the maximum amounts of precipitation at different width of rain drop spectra at $50 < x < 170$ km and $-60 < y < 30$ km

№	*R*	*a*	*t*, h				$\sum_0^{12}$
			3	6	9	12	
1	46	1,0	0,0	0,8	1,2	1,4	3,4
2	69	1,1	0,1	1,6	5,6	9.4	18
3	86	1,2	0,0	3,6	17	25	46
4	215	1,3	0,1	3,5	21	47	62
5	452	1,4	0,2	5,0	36	56	97
6	1660	1,6	0,1	5,2	23	57	85
7	5550	1,8	0,1	3,7	23	50	77
8	16400	2.0	0,1	2,9	24	52	79

In Table 4 it is shown precipitation amounts in the epicenters at the different temperature on the earth. Layering height for calculation of vertical movements was launched. Catastrophic value amounts of rain in 12 hours were obtained only taking into account the processes of coagulation. Increased upper limit of computer networks did not increase the amounts of precipitation. Obviously, in the warm front the rain drops played the crucial role in formation of catastrophic rainfall amounts. Seeding by small crystals from tops of clouds of water and mixed layers strengthened a competition of precipitation particles and reduced their number only.

Table 4

Precipitation sums evolution at different variation of the surface temperature at $50 < x < 170$ and $-60 < y < 30$ km. T_a is parameter in formula (4), $T_a = 6$ h. c_1, c_2 as in Table 1. 2c presented the permanent fall of temperature

№	a_T	*ds*	c_1	c_2	*t*, h				
					3	6	9	12	$\sum_0^{12}$
1	2	200	0	0	0,1	2,2	3,0	18	23
2	0	200	0	0	0,1	9,4	4,2	0,2	14
3	2	200	1	1	1,9	7,9	30	24	64
4	0	200	1	1	1,2	13	30	5,2	49
5	2	150	0	0	1,3	16	16	13	45
6	0	150	0	0	1,3	7,1	2,5	9,3	20
7	2	150	1	1	6,9	50	44	30	131
8	0	150	1	1	5,8	56	53	17	132
9	2c	150	1	1	6,9	54	93	217	371

Additional temperature change on the ground under daily course lead to changes of precipitation amounts, but it is difficult to indicate a direct relationship according to calculations. The results are more evident for the Case 9 in Table 4 when additional decrease in temperature on earth was carried out evenly over the estimated time of 2^{o}/h. Rainfall increased in catastrophic already after 6 hours and kept this trend permanently.

From Fig. 7 shows that the additional decrease in temperature increases the number of centers of heavy precipitation in all cases, the presence of coagulation process and without them. As shown in Fig.7 region was in the zone of the warm front, the sharp decrease of temperature does not appear to be directly over the ridge and only individual precipitation cells were noted (Fig. 3, 4). Very heavy precipitation fall out on both sides of the ridge. In the East of Carpathian Mountains it was highest.

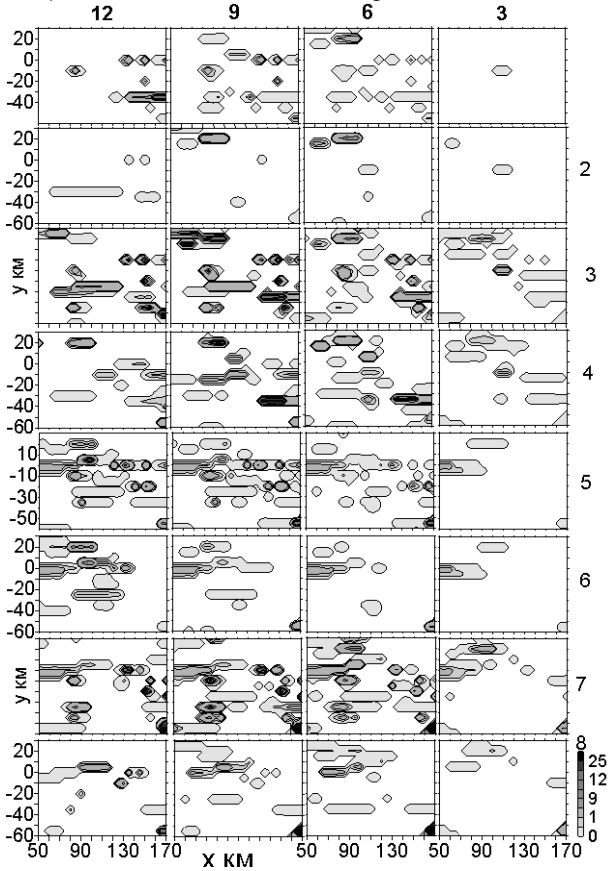

Fig. 7 Evolution of rainfall amounts at the different surface temperature variations
Numbers of rows as Table 4

Excluding processes of coagulation practically excluded the strong rainfall centers in Carpathian at a_T = 0. Comparing Case 4 with Case 6, it should be noted that processes of precipitation formation above tropopause showed themselves the most active and led to a decrease in the maximum amounts of precipitation, but to increase the number of cells with precipitation.

Competing ice phase significantly reduced the catastrophic precipitation intensity and caused widening them by area. Distribution pattern of precipitation for June 2000 GMT closest to real.

Conclusions

A series of numerical experiments carried out to study the influence of different mechanisms of formation of clouds and precipitation on the evolution of cumulus cells capable of giving heavy precipitation.

Numerous experiments have shown that the bulk of precipitation is formed in supercooled layers located above the zero - isotherm, whose height exceeded 3 km. In order to precipitation particles reached to the ground it is necessary the presence of saturated layers under the clouds or the fall velocity of particles is fast enough for it did not evaporate in unsaturated layer.

The key parameters that could lead to the formation of catastrophic rainfall was found as follows: 1) Presence of ice saturation in initial time. 2) Appropriate temperature gradients that create a favorable condition for the formation of condensation nuclei and ice nuclei activation. 3) Enough mass of free for sublimation of water vapor that could ensure the growth of cloud particles to the particle precipitation. 4) Coagulation processes provide opportunity to grow of precipitation particles to the big sizes capable to support the fall velocity of the necessary speed to fly unsaturated layers and reach to the ground. 5) The presence of mechanisms of the formation of drop and crystal spectra of optimal width, capable to provide a rapid fall of precipitation particles in unsaturated layers. 6) The presence of saturated layers under clouds. 7) Sufficient intensity of formation mechanisms of ice cloud particles and ice precipitation. 8) Coagulation of small drops with the large drops as the most probable formation mechanisms of catastrophic rainfall can be called. 9) With the most productive ice formation processes there were found the freezing processes. 10) In certain conditions, very heavy rainfall could be caused by the water vapor redistribution of drops on the crystals. 11) Most likely to receive catastrophic fallout when one phase prevails in the formation of precipitation. 12) The presence of multiple equal mechanisms of precipitation formation generates competition between particles of different nature when consumed for free sublimation of water vapor and the probability of catastrophic rainfall formation decreases.

References

1. Belyi, T.A., Dudar, S.M., Pirnach, A.M., 2009. Numerical studies of the effects of different mechanisms of atmospheric precipitations on the evolution of mesoscale cloud formation, which caused strong rainfalls in Carpathians, 21-29 of July 2008. Geophysical Journal. Vol. 31. pp.107-124.
2. Boyko, V.M, Kulbida, M.I, Susidko, M.N., 1999. A famous rain flood on the rivers of Zakarpattya region in November of 1998. Trudy UHMI vol. 247. pp. 91-101.
3. Bujkov, M.V, 1978. Numerical simulation of stratiforms clouds theory. Obninsk., 68 pp.
4. Muchnik, V.M., 1961. Approximate assessment of water content cumulus-congestus clouds. Research clouds, precipitation, and lightning electricity. Reports of 6-th interdepartmental conference. Moscow: USSR Academy of Sciences. pp. 204-209
5. Pirnach, A.M., Zabolotska T.N., Pidhurska, V.M, Shpital, T.N., 2002. Numerical and experimental researches of the frontal systems which caused the dangerous phenomena over Ukraine. Trudy UHMI. vol. 250. pp. 42-60.
6. Pirnach, A.M., 2004. Simulation of strong frontal rainfall for plane and complex terrain. Trudy UHMI. vol. 253. pp. 37-50.
7. Pirnach, A.M., Dudar, S.M., Shpyg, V.M., 2006. Numerical modeling of the frontal cloud systems which accompanied a strong flood in Carpathians in November 1998. Trudy UHMI. vol. 255. pp. 5-25.
8. Pirnach, A.M., 2007. Modeling of evolution of mesoscale cloud formations over Carpathian. Trudy UHMI. vol. 256. pp.19-43.
9. Pirnach, A.M., 2008: Numerical modeling of clouds and precipitation in atmospheric frontal systems. Kyiv, Nika-Center, 294 pp.
10. Shishkin, N.S., 1964. Clouds, precipitation and thunderstorm electricity. Leningrad, Gidrometeoizdat. 280pp.
11. Heavy Precipitation in Eastern Carpathian and Microphysical Mechanisms of their Formation. Pirnach, A.M., Belyi,T.A., Shpyg, V.M., Dudar, S.N. The 13th Conference on Cloud Physics. 13th Conference on Atmospheric Radiation (28 June–2 July 2010) of American Meteorological Society. P2.85. http://ams.confex.com/ams/13CldPhy13AtRad/techprogram/paper_170141.htm